THE VALUE OF MRI IN SPINAL PATHOLOGIES : BASIC PRINCIPLES AND RECENT ADVANCES

H. B. DİREN *

ABSTRACT:

The multiplanar capability of MRI has markedly benefited the study of the spine. T_1-weighted images yield morphological images of the cord and roots contrasting against the low-intensity CSF (4) (Fig. 1). T_2-weighted images provide different types of information; the ***"myelographic effect"****, in which CSF appears very bright, delineates nervous structures (spinal cord and roots), as well as ligaments, which remain dark or gray. In this article, the basic principles of MRI and recent advances in the evaluation of spinal pathologies have been presented and current literature has also been reviewed.*

Key Words: *Magnetic Resonance Imaging, Spine Pathology*

The multiplanar capability of MRI has markedly benefited the study of the spine. The T_1-and T_2-weighted images allow direct visualization of the spinal cord besides the osseous structures of the spine, which has previously not possible in a noninvasive fashion (1-3). Meanwhile, the sagittal plane allowing for visualization of a whole segment of the spine (approximately ten vertebral bodies) is very helpful.

Recent advances on MRI technic, helped us for more effective use of this modality in the evaluation of different diseases. In this article, the basic principles of MRI and recent advances in the evaluation of spinal pathologies have been presented and current literature has also been reviewed.

T_1-WEIGHTED IMAGES

T_1-weighted images yield morphological images of the cord and roots contrasting against the low-intensity CSF (4) (Fig. 1). The vertebral bodies have two different signal intensities: the cortical bone yields a very low signal intensity due to the lack of mobile protons, whereas the cancellous bone produces a high signal intensity due to the presence of fatty marrow within it. This type of sequence confuses cortical bone, ligaments, and CSF and is not appropriate to study the spinal canal caliber as it may mislead for normality.

The intervertebral discs appear homogeneous and slightly more intense than the vertebral bodies. With T_1-weighted gradient echo technique those relative intensities are modified because faaty marrow appears less intense than with spin echo; cancellous bone presents the same signal intensity or lower signal intensity than discs. The use of surface coils producing improvement in spatial resolution allows for differentation between periependymal gray matter and white matter tracts (6). This is usually more striking on axial slices. At the cervical level, axial slices also allow for visualization of anterior and posterior nerve roots (7). Lumbar spine benefited from oblique slices parallel to the discs to better studythe nerve roots in the lateral recesses and in the foramina (7, 8). Parasagittal slices through the foramina show the nerve roots within the epidural fat, joined with vascular elements (4).

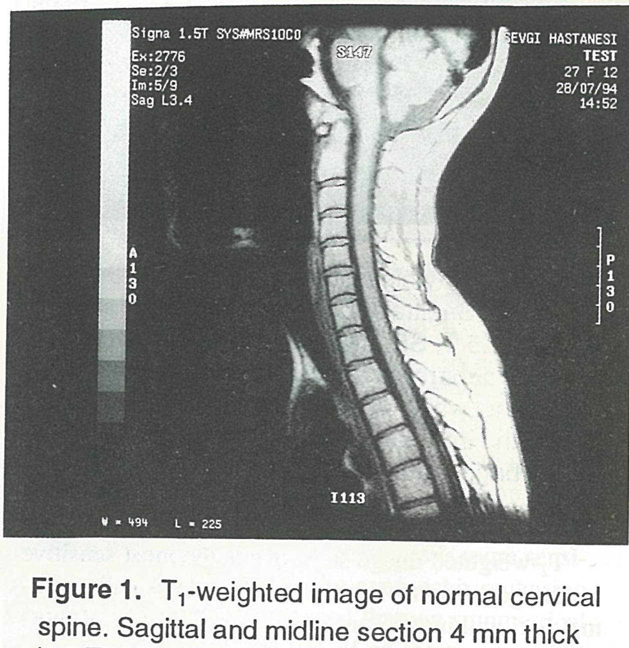

Figure 1. T_1-weighted image of normal cervical spine. Sagittal and midline section 4 mm thick (1.5 T, SE 600/15). CSF is lower intensity when compared with the cord.

* Sevgi Hospital, Ankara, TÜRKIYE

T_2-WEIGHTED IMAGES

T_2-weighted images provide different types of information; the **"myelographic effect"**, in which CSF appears very bright, delineates nervous structures (spinal cord and roots), as well as ligaments, which remain dark or gray. This sequence allows for the best visualization of the interface between CSF and spinal canal. The T_2-weighted contrast of bodies and discs shows lower intensity of cancellous bone due to short T2 of fat. Intervertebral discs appear brighter and the intensity is higher in hydrated discs. The hydration of the disc is more important in the lumbar than in the cervical region. It also decreases with age. It is sometimes possible to demonstrate a hypointense band within the disc, the intranuclear cleft, corresponding to a fibrous septum extending from the annulus and separating the nucleus pulposus in two parts (Fig. 2). This cleft is present in most patients older than 20 and is mainly visible in the lumbar spine (9, 10).

Figure 2. T_2-weighted image of normal thoracal spine. Sagittal and midline section 4 mm thick (1.5 T, SE 300/105). CSF is bright and easily separeted from the cortical bone and ligaments which are hypointense. The nucleus and the internal segment of the annulus are very bright and intraunclear cleyts with in the discs are clearly.

T_2-weighted image sequence is the most sensitive to changes in water content. It can show small abnormal foci within the cord even in the absence of morphological changes on T_1-weighted images (e.g., multiple sclerosis, transverse myelitis, cervical mylopathy, cord contusion) (Fig. 3).

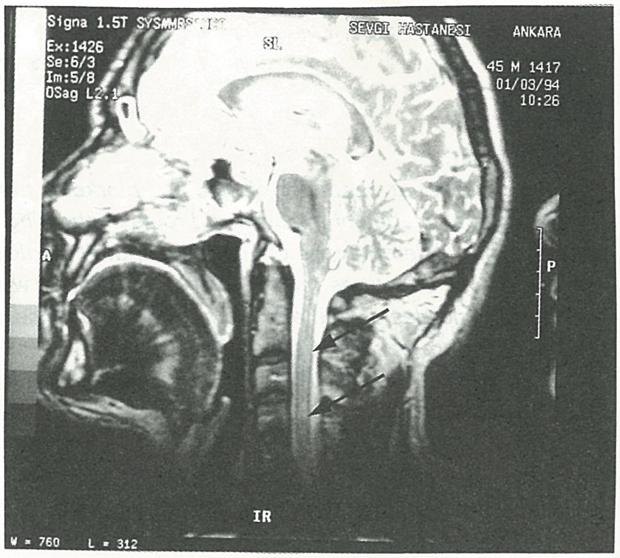

Figure 3. Multiple sclerosis of cervical spinal cord. T_2-weighted sagittal image shows clearly bright foci within the cord (arrows).

The T_2-weighted images in the spine are sometimes degraded by artifacts due to CSF pulsation and to the motion related to the cardiac and respiratory movements. These will be detailed in the next paragraph. Cardiac gating seems to improve the images and overcome these artifacts. It is necessary in the cervical and thoracic but not in the lumbar spine, where the pulsations of the CSF are not as important.

Gradient echo images are very useful in obtaining myelographic-type images without requiring cardiac gating. This is easily performed in the cervical, upper thoracic, and lumbar spine (Fig. 4). At the level of the heart these sequences produce inconstant results. Sagittal images, even in fewer number as obtained with this technique, are satisfactory for a narrow structure such as the spine. The axial images produce high signal intensity in the CSF and epidural veins, allowing for an excellent visalization of the foramina and reliable depiction of subarachnoid space compression (Fig. 5). These images are acquired faster and allow for excellent delineation between spine and CSF without requiring cardiac gating. However, their reliability for diagnosis of long T_2 foci inside the spinal cord is still controversial as compared to the lang TR, long TE se-

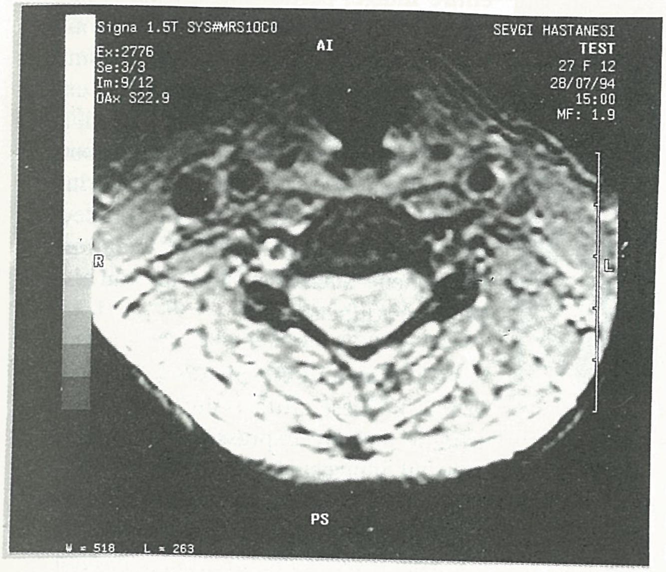

Figure 4. Axial Gradient-echo image of normal cervical spine (1.5 T, GRE 57/8/15°). This sequence allows for the best visualization of the interface between CSF and spinal canal and the white and the central gray matter can be differentiated within the word.

Figure 5. Axial T_2-weighted images of lumbar spine at the level of L5-S1. Posterior protrusion of intervertebral disc and the compression of anterior subaraknoid space are clearly seen.

quences if the spinal cord is morphologically intact (11-14).

EXAMINATION TECHNIC OF THE SPINE

MRI examination of the spine most often includes:

1. a sagittal morphological T_1-weighted image with thin sections (4mm),
2. a sagittal T_2-weighted image,
3. axial or oblique T_1-weighted images as needed (7)

The T_1-weighted images my be performed either with spin echo or gradient echo images with a long flip angle (60° to 90°). The T1 weighting requires a short TR (300 to 600 msec) and a short TE (less than 20 msec). The multislice mode allows a relatively small number of slices to be performed during the short TR but these sections are most often enough to study the whole width of the canal in the sagittal plane even when using thin sections (15, 16). The use of thin sections is paramount due to the small size of the cord. Sections of 3 to 4 mm in width are recommended in the cervical and thoracic spine. In the lumbar spine section of 5 mm are acceptable. Contiguous sections must be used if the gradient echo technique is performed because it produces strictly vertical slice profiles. Therefore, even small gaps between slices can miss lesions.

With spin echo, slice profiles are less strictly vertical and a 1-mm gap is acceptable. Threedimensional (3-D) acquisitions are currently available in new MR units made by after the year of 1990 and should become more routinely used as the reconstruction times decrease (17). Additionally, although 3-D technique has better signal-to-noise ratio it has lower contrast than 2-D technique applied to the spine (18).

The T_2-weighted images may be performed using gradient echo techniques or spin echo sequences. When spin echo sequences are used, cardiac gating is helpful in the cervical and thoracic region (19). TR of 1,800 to 3,000 msec may be used and the TE should be of 50 to 90 msec using a double echo technic.

Certain manufacturers have introduced asymmetrical echoes. Thus, one can obtain a first echo that is relatively T_1-weighted and a second echo with relative T_2-weighting using an intermediate TR of approqimately 1,000 msec. This markedly decreases the acquisition time. However, this technique is more sensitive to flow artifacts since the even echo rephasing phenomenon is less proneunced than on symmetrical echoes. Furthermore, the use of an intermediate TR

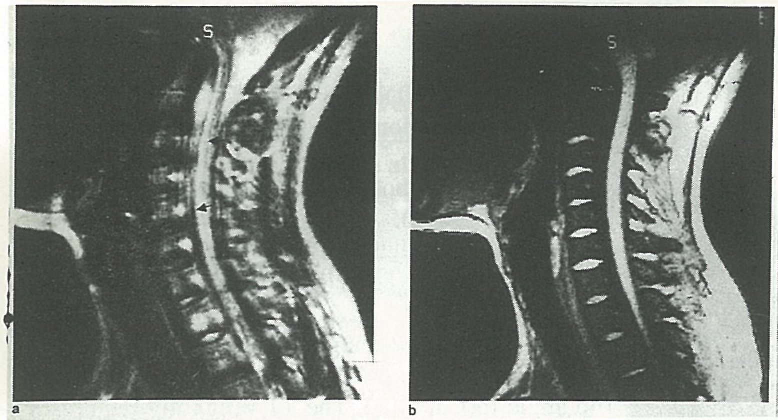

Figure 6. Motion artifacts mimicking syringomyelia.
a) The image artifact is due to phase shift secondary to patient motion and a low intensity intramedullary area of high signal intensity (arrows) could mimic a syrinx
b) The sagittal T_1-weighted GRE image demonstrates no intramedullary pathology.

decreases the signal-to-noise ratio especially on the second echo. Thus, this method is mainly used on the high field (1,5 T) systems that have additional signal-to-noise due to their high field strength.

The T_2-weighted sequences using gradient echo can be used as an alternative to the long TR sequences (20). In the cervical and lumbar region, the image quality is generally sufficient for a good examination.

FITFALLS AND ARTIFACTS

MRI is susceptible to numerous artifacts (21, 22). Some are common and easily identifiable; others are more discrete and may be mistaken for pathology. Artifacts reflect the complexity of MRI. Their unterstanding requires some knowledge of MRI technology and physics. Artifacts can be separated somewhat artificialy into artifacts due to the patient or due to the MRI technique.

Patient-Related Artifacts: Patient-related artifacts include the artifacts due to patient motion during the examination, artifacts of the metallic implants, and artifacts due to the contrast medium.

Intentional or Unintentional Patient Motion (23): These artifacts degrade the image in the direction of the phase-encoding gradient. One can see either a blurred appearance of the anatomical interfaces or alternation of hyper- and hypointense bands (phantom images or harmonics) that are projected over the entire image, particularly in the spine. On the sagittal images these can mimic intramedullary cavities or neoplasm (Fig. 6); the axial images usually can exclude the presence of a syrinx. Thus, it is important for the patient to be in a comfortable position so that motion during the examination can be minimized. Some patients will require sedation. Movements such as swallowing can also produce artifacts.

Cardiac and Respiratory Motion (24, 25): These artifacts are easily identifiable and are expressed by multiple parallel images of the thoracic walls (harmonics), which are projected on the adjacent organs or outside the body (Fig. 7). The artifacts due to cardiac motion (26) are particularly troublesome for the study of the thoracic spine because they can produce phantom images projecting over the cord mimicking intramedullary pathology. The reversal of the phase-and frequency-encoding gradients can help palliate this difficulty. Cardiac gating also decreases these artifacts.

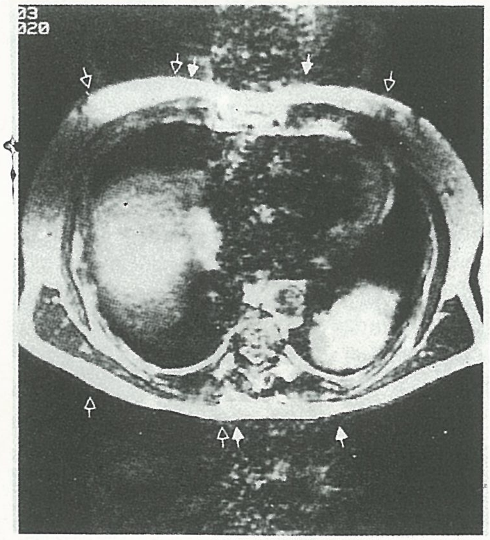

Figure 7. Cardiac and respiratory artifacts. Respiratory artifact (open arrows) and cardiac artifacts (white arrows) are seen in axial T_1-weighted image.

Physiologic Motion of Body Fluids: These artifacts are created by blood flow and CSF pulsation. The CSF motion is complex, depending on anatomical and physiologic factors. Among them the pulsations transmitted by the cardiovascular system play a major role in the appearance of the MRI signal. For this reason the study of flowing blood and CSF motion can be performed simultaneously. Two types or artifacts need to be considered. The first type is directly related to flow phenomena (27): decreased signal at high speed due to turbulent flow and dephasing of moving spins on odd echoes, and high signal intensity due to entrance slice phenomenon, spin rephasing on even echoes, and pseudogating during diastole and systole. Two artifacts at the level of the cord are worth mentioning since they can be particularly deceiving. The first is due to an entrance slice phenomenon (28). At the level of the first section (and more rarely on the last one) of the axial image of a multislice T_1-weighted sequence, CSF appears hyperintense and may mimic a tumor or a disc herniation. In fact, this high signal intensity is due to the entrance in the plane of section of unsaturated protons. One can exclude an abnormality by performing an additional sequence in a different plane.

The second artifact is due to the dephasing of spins secondary to turbulence. It is seen when the plane of section is parallel to the direction of flow (sagittal plane when imaging the spine). It is due to the fact that CSF flows more rapidly where the busarachnoid sapces are narrow, in particular in the cervical thoracic region when compared to the lumbosacral region. Out of these conditions, the protons undergo different accelerations and the phase angles become variable. The 180° refocusing pulsis cannot refocus them anymore, hence the high intensity of the CSF on T_2-weighted images in the lumbar spine in comparison with the thoracic spine; this may suggest intradural pathology. This artifact is relatively rare in the spine. However, it is common in the aqueduct of Sylvius, which appears usually as a hypointense area on the T_2-weighted images (29).

In the second group are included the artifacts resembling cardiac and repiratory artifacts; they also are phantom images projected outside the vessels and subarachnoid spaces on the adjacent structures, in particular, along the spinal cord itself. Here, too, they are noticed along the phase-encoding direction. To correct the artifacts due to CSF pulsation, one can severse the phase and frequency-encoding direction (30), or use cardiac gating. This technical solution makes sense since the artifacts are related to the consequence of the cardiovascular pulsations on the CSF; furthermore, it is easily implementable (EKG gating or photoplethysmography) (31). However, these methods cannot always correcty the artifact in the posterior subarachnoid spaces of the thoracic region. Here, these artifacts often mimic vessels in the subarachnoid space, mimicking an arteriovenous malformation or a dural fistula with medullary venous drainage (Fig. 8). Axial images are required to exclude such pathology.

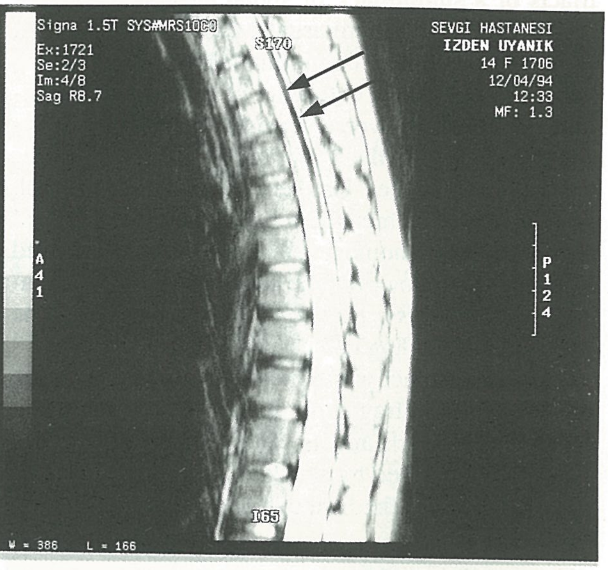

Figure 8. CSF flow mimicking dilated subaraknoid vessels in the thoracic spine. Sagittal T_2-weighted image shows hypointense artifacts mimic vessels posteriorly to the thoracic cord (arrows).

Metalic Artifacts (32): A metalic implant poses two types of problems: potential danger to the patient due to its movement in the magnetic field, an distortion of the image due to the effect of the implant on the local magnetic field homogeneity and to its marked absorption of elektromagnetic waves.

The metalic implants (e.g., hip prosthesis, dental prosthesis, orthopedic plates and screws) do not constitute a contraindication to MRI. There are, however, certain absolute contraindications that have to be routinely creened for: cardiac pacemakers, intracranial aneurysm clips, and metallic fragments that can be mobilized by the magnetic field, such as foreign intraocular bodies or bullet fragments. Vascular clips on the dura do not constitute a contraindication if they are far enough from the sinuses. The artifact is smaller than the artifact produced on CT and it is possible to obtain a diagnostic-quality image except in a small area around the prosthesis. Visualization of the spine and spinal cord is usually not impaired unless the implants are located in the same section as the cord. The largest artifacts are produced by pure ferromagnetic elements (iron, nickel, chrome, cobalt) or when these elements are used in alloys. The non-ferromagnetic metals aluminum, gold, silver produce onl limited artifacts or a simple lack of signal at the level of the prosthesis. Artifacts are usually easy to recognuze: a central hypointense area surrounded by a hyperintense border with variable deformity of the adjacent structures. Artifacts are worse when the signal-to-noise ratio is low, e.g., on the T_2-weighted images or on the gradient echo images. Gradient echo images are much more sensitive to metallic artifacts because the local magnetic field inhomogeneities are not compensated by a spin echo; however, the artifact deforms the adjacent structures less. Thus, one can use one technique or another depending upon each particular situation.

Another artifact worth mentioning is the presence of metalic microfragments from surgical drills and other surgical instruments. These fragments are too small to be detected by standard radiographs but distort the magnetic field enough to produce an artifact (33).

Artifacts Due to Pantopaque (34): Old oil-based mylographic material is fonud in patients who had these studies before the introduction of water-soluble contrast. They have similar signal intensity to fat, and may mimic a lipoma. The diagnosis is obvious on a plain film or a CT scan.

Chemical Shift Artifact (35): This artifact is due to the fact that the resonant frequency of hydrogens bound to water is slightly superior to that of the resonant frequency of hydrogens in fat. The 2-D FT technique most commonly used for the image reconstruction translates these differences in frequency between different tissues in different spatial locations. This results in an apparent misregistration at the border between structures with a high fat content and structures with a high water content. In the spine, this artifact is consistently seen at the junction between the intervertebral discs (high water content) and the vertebral bodies (high fat content). This artifact can be confirmed by reversing the phase- and frequency-encoding direction and demonstrating shifting of the artifact with the frequency-encoding axis.

Ailasing artifact (36): This artifact seen when the size of the object to be visualized is larger than the field of view used or when the patient is not centered in the magnet. It appears by an infolding of a peripheral part of the patient into the center of the image. If this projection occurs in an area of the field of view which is already filled, a superimposition occurs that prevents an accurate analysis.

Truncation Artifact (6, 7): This artifact occur at the interfaces between different structures and appears as multiple hypo- and hyperintense bands parallel to the interface between two regions of very different signal intensity. It is due to the difficulty of the Fourier transformation to accurately represent a sudden transition in signal. In the spine it is usually seen on sagittal T_2-weighted images where CSF is of high intensity and the adjacent structures, in particular the cord, are hypointense; it can mimic then an intramedullary cavity (Fig. 9). The correct diagnosis is made on the axial images with T_1-weighting.

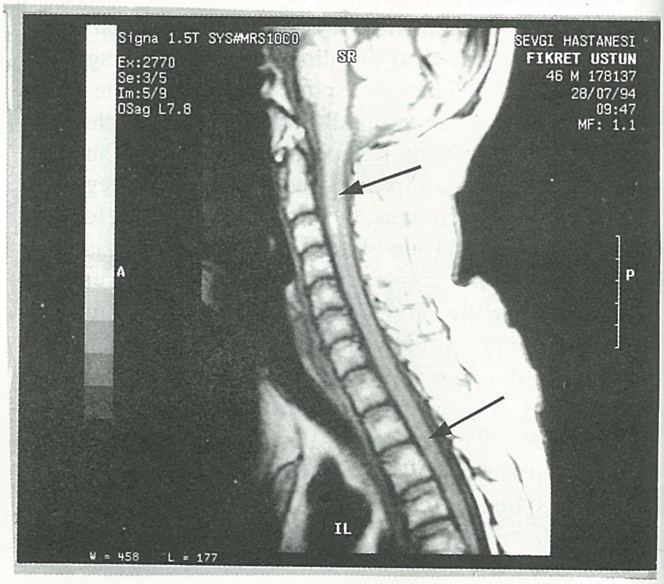

Figure 9. Truncation artifact. Sagittal T_1-weighted image shows hypointense intermedullary signal (arrows) paralleling the interface between the CSF and the cord and simulating syrinx.

Signal Inhomogeneity (38): This type of artifact should be distinguished from the normal asymmetry resulting from the use of a surface coil; in this case on can see a progressive decrease of the signal intensity from the patient's skin toward the deeper soft tissues. Any other difference of intensity in a part of an image where one does not except it is artiactual. It may be due to a defect in field homogeneity transmitted by the coil or the filters or a gradient failture.

Radio-Frequency Interferences (36): These interferences can have an internal origin (different parts of the machine) or external (poor radio-frequency insulation). They are usually easy to recognize, and the image has a striped appearance when the bandwidth of the noise is wide, or bands of signal traversing the entire image along the frequency-encoding direction when the noise has a welldefined frequency.

FUTURE EXPECTATIONS

In recent years, the most important researches helding on MRI are detecting the findings during the function of the examined body portion. These are also trying in spine during hyperextention and hyperflexion for detecting the disc herniation which produce compressive mylopathy. In the way of neutral position sometimes this kind of finding can not be detect. In our center we managed to examine of cervical spine during the movement from hyperextention of hyperflexion, we called this new application as "kinematic MRI". When we compared the findings of kinematic MRI with routine technic we noticed that there ca be some differences between them. Such as some normal appearences in MR examination of neutral position change in this kinematic application (Fig. 10). We hope that in the near future such kind of applications will be develope and objective criterias will be create for correct diagnosis.

REFERENCES:

1. Balériaux, D., Deroover, N., Hermanus, N., Segebarth, C.: MRI of the spine. Diagn. Imag. Clin. Med., 55: 66-71, 1986.
2. Haughton, V.M.: MR imaging of the spine. Radiology, 166: 297-301, 1988.
3. Stark, D.D., Bradley, W.G.: Magnetic resonance imaging. St. Louis: C.V. Mosby, 1988.
4. Flannigan, BD., Lufkin, R.B., McGlade, C., Winter, J., Batzdorf, U., Wilson, G., Rauschning, W., Bradley, W.G.: MR imaging of the cervical spine: neuroavascular anatomy. A.J.N.R., 8: 27-32, 1987.
5. Turner, R., Le Bihan, D., Maier, J., Vavrek, R., Hedges, L.K., Pekar, J.: Echoplanar imaging of introvoxel incoherent motions. Radiology, 177: 407-414, 1990.

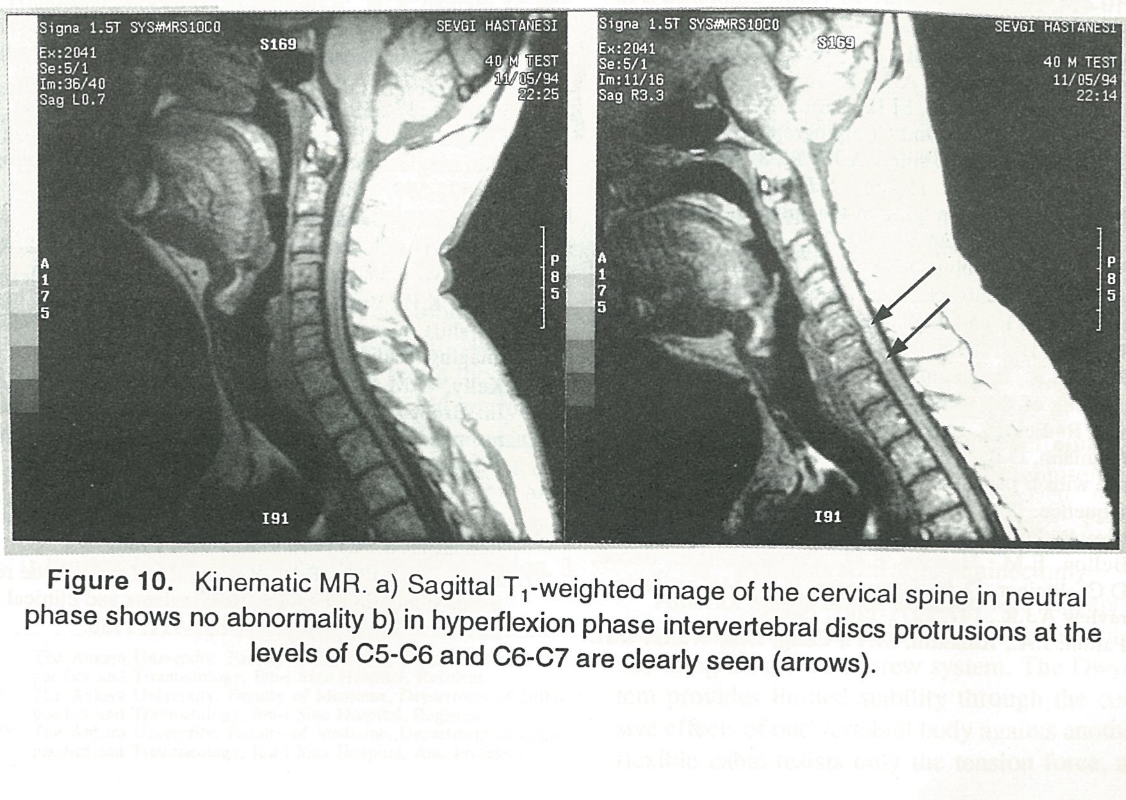

Figure 10. Kinematic MR. a) Sagittal T_1-weighted image of the cervical spine in neutral phase shows no abnormality b) in hyperflexion phase intervertebral discs protrusions at the levels of C5-C6 and C6-C7 are clearly seen (arrows).

6. Czervionke, L.F., Daniel, D.L., Ho, P.S.P., Yu, S., Pech, P., Strandt, J.A., Williams, A.L., Haughton, V.M.: The MR appearance of gray and white matter in the cervical spinal cord. A.J.N.R., 9: 557-562, 1988.
7. Edelman, R.R., Stark, D.D., Saini, S., Ferrucci, J.T., Dinsmore, R.E., Ladd, W., Brady, T.J.: Oblique planes of section in MR imaging. Radiology, 159: 807-810, 1986.
8. Reicher, M.A., Gold, R.H., Halbach, V.V., Rauschning, W., Wilson, G.H., Lufkin, R.B.: MR imaging of the lumbar spine: anatomic correlations and the effects of technical variatonis. A.J.R., 147: 891-898, 1986.
9. Aguila, L.A., Piraino, D.W., Modic, M.T., Dudley, A.W., Duchesneau, P.M., Weinstein, M.A.: The intranuclear cleft of the intervertebral disk: magnetic resonance imaging. Radiology, 155: 155-158, 1985.
10. Pech, P., Haughton, V.M.: Lumbar intervertebral disk: correlative MR and anatomic study. Radiology, 156: 699-701, 1985.
11. Enzmann, D.R., Rubin, J.B.: Cervical spine: MR imaging with a partial flip angle, gradient-refocused pulse sequence. Part II. Spinal cord disease. Radiology. 166: 473-478, 1988.
12. Hedberg, M.C., Drayer, B.P., Flom, R.A., Hodak, J.A., Bird, C.R.: Gradient-echo (GRASS) imaging in cervical radiculapathy. A.J.N.R., 9: 145-151, 1988.
13. Katz, B.H., Quencer, R.M., Hinks, R.S.: Comparison of gradient-recalled echo and T2-weighted spin-echo pulse sequences in the intramedullary spinal lesions. A.J.N.R. 10: 815-822, 1989.
14. Watanabe, A.T., Teitelbaum, G.P., Lufkin, R.B., Tsuruda, J.S., Jinkins, J.R., Bradley, W.A. Jr.: Gradient-echo MR imaging of the lumbar spine: comparison with spin-echo technique. J. Comput. Assist. Tomogr. 14: 410-414, 1990.
15. Hyman, R.A., Edwards, J.H., Vasirca, S.J., Stein, L.: 0.6 T MR imaging of the cervical spine: multislice and multiecho techniques. A.J.N.R., 6: 229-236, 1985.
16. Karnaze, M.G., Gado, M.H., Sartor, K.J., Hodges, F.J.: Comparison of MR and Ct mylography in imaging the cervical and thoracic spine. A.J.N.R., 8: 983-989, 1987.
17. Gallimore, G.W., Harms, S.E.: Selective three-dimensional MR imaging of the spine. J. Comput. Assist. Tomogr. 11: 124-128, 1987.
18. Enzmann, D., Rubin, J.B.: Short TR, variable flip anlge, gradient-echo scans of the cervical spine: comparison of 2DTF and 3DFT techniques, Neuroradiology, 31: 213-216, 1989.
19. Rubin, J.R., Enzmann, D.R., Wright, A.: CSF-gater MR imaging of the spine: theory and clinical implementation. Radiology, 163: 784-792, 1987.
20. Enzmann, D.R., Rubin, J.B.: Cervical spine: MR imaging with a partial flip angle, gradient-refocused pulse sequence. Part I. General considerations and disk disease. Radiology, 166: 467-472, 1988.
21. Bellon, E.M., Haacke, E.M., Coleman, P.E., Sacco, D.C., Steiner, D.A., Gangarosa, R.E.: MR artifacts: a review A.J.R., 147: 1271-1281, 1986.
22. Patton, J.A., Kulkarni, M.V., Craig, J.K., Wolfe, O.H. Price, R.R., Partain, C.L., James, A.E.: Techniques pitfalls and artifacts in magnetic resonance imaging. Radiographics, 7: 505-519, 1987.
23. Schults, C.L., Alfidi, R.J., Nelson, A.D., Kopiwoda, S.Y., Clampitt, M.E.: The effect of motion on two dimensional Fourier transformation magnetic resonance images. Radiology, 152: 117-121, 1984.
24. Ehman, R., McNamara, M.T., Brasch, R.C., Felmiee, J.P., Gray, J.E., Higgins, C.B.: Influence of physiologic motion on the appearance of tissue in MR images. Radiology, 159: 777-782, 1986.
25. Pele, N.J., Glover, G.H., Charles, H.C.: Respiration artifacts in MRI. In: Proceedings of the Society of Magnetic Resonance in Medicine. Aug. 19-23, London, 1985.
26. Perman, W.H., Moran, P.R., Moran, R.A., Bernstein, M.A.: Artifacts from pulsatile flow in MR imaging. J. Comput. Assist. Tomogr. 10: 473-483, 1986.
27. Bradley, W.G.: Magnetic resonance appearance of flowing blood and cerebrospinal fluid. In: Brant-Zawadzki, M., Norman, D., eds. Magnetic resonance imaging of the central nervous system. New York, Raven Press: 83-96, 1987.
28. Williams, D.M., Meyer, C.R., Schreiner, R.J.: Flow effects in multislice, spin-echo magnetic resonance imaging. Model, experimental verification, and clinical examples. Invest. Radiol., 22: 642-650, 1987.
29. Citrin, C.M., Sherman, J.L., Gangarosa, R.E., Scanlon, D.: Physiology of the CSF flow-void sign: modification by cardiac gating. A.J.N.R., 7: 1021-1024, 1986.
30. Enzmann, D.R., Griffin, Ch., Rubin, J.B.: Potential false-negative MR images of the thoracic spine in disk disease with switching of phase- and frequency-encoding gradients. Radiology, 165: 635-637, 1987.
31. Laakman, R.W., Kaufman, B., Han, J.S., Nelson, A.D., Clampitt, M. O'Block, A.M., Haaga, J.R., Alfidi, R.J.: MR imaging in patients with metallic implants. Radiology, 157: 711-714, 1985.
32. Heindel, W., Friedmann, G., Bunke, J., Thomas, B., Firsching, R., Ernestus, R.I.: Artifacts in MR imaging after surgical intervention, J. Comput. Assist. Tomogr., 10: 596-599, 1986.
33. Braun, I.F., Malko, J.A., Davis, P.C., Hoffman, J.C., Jacobs, L.H.: The behavior of Pantopaque on MR: in vivo and in vitro analyses. A.J.N.R. 7: 997-1001, 1986.
34. Soila, K.P., Viamonte, M.Jr., Starewicz, P.M.: Chemical shift misregistration effect in magnetic resonance imaging. Radiology, 153: 819-820, 1984.
35. Kelly, W.M.: Image artifacts and technical limitations. In: Brant-Zawadzki, M., Norman, D., eds. Magnetic resonance imaging of the central nervous system. New York, Raven Press: 43-82, 1987.
36. Czervionke, L.F., Czervionke, J.M., Daniels, D.L., Haughton, V.M.: Characteristic features of MR truncation artifacts. A.J.N.R. 9: 815-824, 1988.
37. Pusey, E., Lufkin, R.B., Brown, R.K.J.: Magnetic resonance imamging artifacts: mechanisms and clinical significance. Radiographics, 6: 891-911, 1986.